GaAs (1 1 1) epilayers grown by MBE on Ge (1 1 1): Twin reduction and polarity

D. Pelati, G. Patriarche, O. Mauguin, L. Largeau, L. Travers, F. Brisset, F. Glas, F. Oehler

GaAs (111) epilayers grown by MBE on Ge (111): twin reduction and polarity

D. Pelati[a,c,d], G. Patriarche[a], O. Mauguin[a], L. Largeau[a], L. Travers[a], F. Brisset[b], F. Glas[a], F. Oehler[a,*]

[a] *Centre de Nanosciences et de Nanotechnologies, CNRS, Université Paris-Sud, Université Paris-Saclay, 10 Boulevard Thomas Gobert, 91120 Palaiseau, France*
[b] *Institut de Chimie Moléculaire et des Matériaux d'Orsay, CNRS, Université Paris-Sud, Université Paris-Saclay, 91405 Orsay, France*
[c] *RIBER SA, 31 rue Casimir Périer, 95870 Bezons, France*
[d] *Institut Photovoltaïque d'Ile-de-France (IPVF), Antony, France*

Abstract

We perform the growth of GaAs (111) epilayers on nominal Ge(111) wafers by molecular beam epitaxy (MBE). The polarity of GaAs is (111)A and homongeneous over the full area, as measured by transmission electron microscopy and high energy electron diffraction. This orientation conflicts with the common growth model for GaAs on Ge(111). Twinned domains are the main defects in our GaAs (111) epilayers. Using cathodoluminescence, we observe that some twin boundaries hold large number of non-radiative recombination centers. During growth, we find that only a narrow domain of As:Ga ratios lead to the growth of smooth and twin-free GaAs (111)A epilayers. At low As:Ga ratio, the surface is rough; while at high As:Ga ratio the epilayers present large densities of twinned domains.

Keywords: Molecular Beam Epitaxy, GaAs, Ge, twin, defect, (111), heteroepitaxy

The heteroepitaxy of III-V materials on group IV substrates presents many challenges. First, most of the III-V and group IV materials are cubic crystals of different lattice parameters, which leads to the formation of dense arrays of dislocations at the III-V / IV-IV interface[1]. Second, the large thermal mismatch between the III-V epilayer and its substrate can lead to cracks after the growth, during the cool down to room temperature[2]. Currently, the direct growth of good quality III-V planar material on silicon is only possible using cunning selective area growth schemes such as InP[3] or InAs[4] on Si (100).

Uniquely, Ge substrates provide a near lattice (-0.9%, a_{GaAs}=5.653Å, a_{Ge}= 5.658Å) and thermal (-2.9%, K_{GaAs}=5.73 10^{-6} K^{-1}, K_{Ge}=5.90 10^{-6} K^{-1}) match to GaAs, so that GaAs/Ge epilayers are relatively immune to the dislocation- and crack-related problems above. However, even in this favorable configuration, the lower symmetry of the GaAs crystal permits the growth of III-V seeds of different epitaxial relationship with the substrate. If the initial GaAs nucleation is uncontrolled, the final epilayer may consist in individual domains, separated by defective interfaces[5]. To avoid this problem, two conditions need to be fulfilled. First, the initial covalent bounds between the GaAs crystal and the Ge substrate need to be uniquely determined: either Ge-Ga or Ge-As. Then, the surface of the substrate needs to present only atomic steps or step bunches which only shift the III-V lattice by one *full* monolayer or multiple thereof. In the case of GaAs on Ge(100) grown by Molecular Beam Epitaxy (MBE), this often requires the use of offcut Ge wafers and specific annealing to produce double-step surfaces[6], which may be combined with dedicated nucleation schemes to initiate the growth[7].

In an attempt to study the simplest model for heteroepitaxy, we investigate here the growth of GaAs(111) on Ge(111) surface. Whereas the Ge(100) surface can present atomic steps of half ($a/4$) or full ($a/2$) monolayer, the (111) surface only presents steps of full monolayer ($a/\sqrt{3}$) or multiple thereof. The Ge(111) surface is also reported to have a strong affinity with As atoms when treated in the appropriate conditions, leading to fully As terminated Ge(111) surface[8, 9]. Combined together, the Ge material and the (111) surface bring respectively the lattice and thermal match, as well as an ideal surface structure and chemistry to control epitaxy the growth GaAs epilayers, including their polarity. The epitaxy of GaAs on Ge(111) is thus a model system for heterogeneous epitaxy[10], yet only

* *Email address:* fabrice.oehler@c2n.upsaclay.fr (F. Oehler)

few reports can be found in the recent literature[11, 12].

1. Experimental

The GaAs epilayers were grown in a Molecular Beam Epitaxy system (MBE, Riber 32) operating in ultra-high vacuum (10^{-10} Torr). Elements were supplied from solid sources: a standard effusion cell for Gallium and a valved cracker cell for As (RIBER VAC500) producing As_4 tetramers (cracker temperature 600°C). Germanium (111) n-type As-doped substrates (from AXT) were loaded without any chemical cleaning and degassed at 350-400°C in a dedicated chamber. The samples were then heated to 610°C, as measured by pyrometry, and exposed to As_4 at 610°C using a beam equivalent pressure (BEP) of 8.9 10^{-6} Torr for a minimum duration of 5 min before the actual GaAs epitaxy. The Ga flux BEP was 1.4 10^{-7} Torr, equivalent to a growth speed of ~1.5 Å.s^{-1} on GaAs (100) substrates. For some samples, a thin AlGaAs marker layer was made with an Al BEP of 5.0 10^{-8} Torr. Different ratios BEP_{As_4} : BEP_{Ga} were used in this study, from 31:1 to 94:1. Reflection

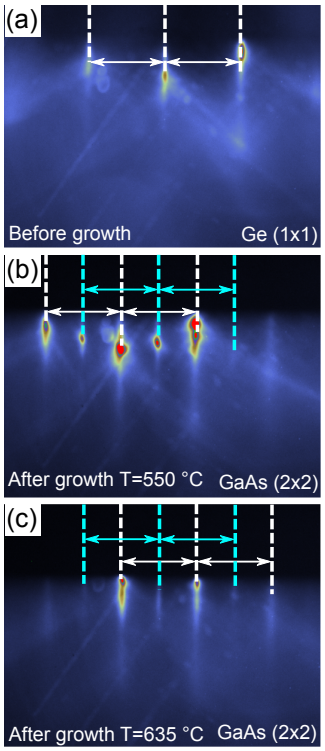

Figure 1: RHEED characterization before and GaAs growth (~9 nm thick) using 62:1 BEP ratio. (a) Ge(111) 1 × 1 before growth. (b) GaAs 2 × 2 at 550°C. (c) GaAs 2 × 2 at 635°C.

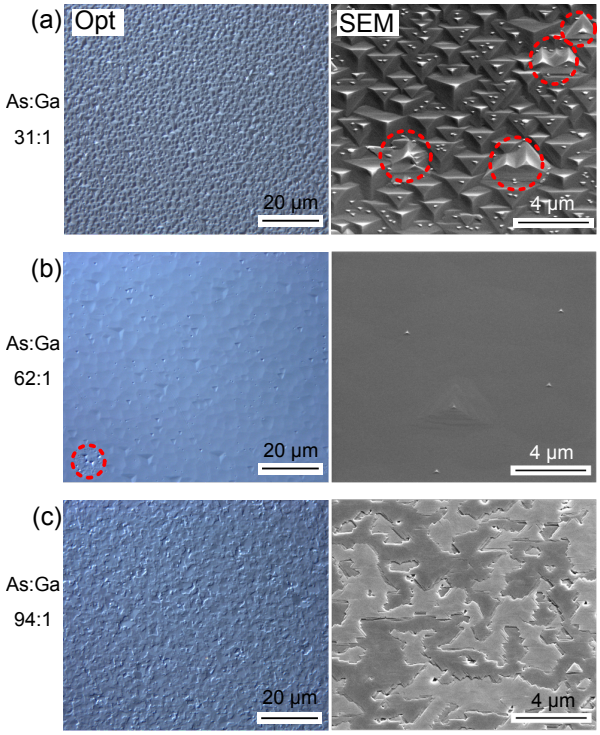

Figure 2: Optical microscopy (Nomarski, left) and SEM view (45° tilt, right) of the surface of GaAs epilayers (~450 nm) on Ge(111) grown with different As:Ga BEP ratios. (a) 31:1 (b) 62:1 (c), 94:1.

High Energy Electron Diffraction (RHEED, 12 kV) was used to characterize in situ the surface reconstructions. The samples were characterized after growth using optical microscopy (Nomarski) and Scanning Electron Microscopy (SEM, FEI Magellan). X-Ray Diffraction (XRD, Rigaku SmartLab with a rotating anode emitting Cu K-alpha doublet radiation) was used to obtain 111 pole figures. Local crystalline orientations were measured using Electron BackScatter Diffraction (EBSD, ZEISS Supra 55 VP with Hikari/OIM TSL EDAX). The layers were also investigated by Transmission Electron Microscopy (TEM, FEI Titan THEMIS) associated with chemical analysis capabilities using Energy Dispersive X-rays Spectroscopy (EDX, Bruker Super-X). Focused Ion Beam (FIB, FEI Scios) was used to prepare the TEM foils. Finally cathodoluminescence (CL) was used to asses the optical properties of selected defects (Attolight Chronos, 6 kV, associated to a Andor Newton CCD).

2. Results

Prior and during the early stage of the growth, we use RHEED to monitor the surface modifications. After the thermal deoxidation of the Ge(111) substrate (above

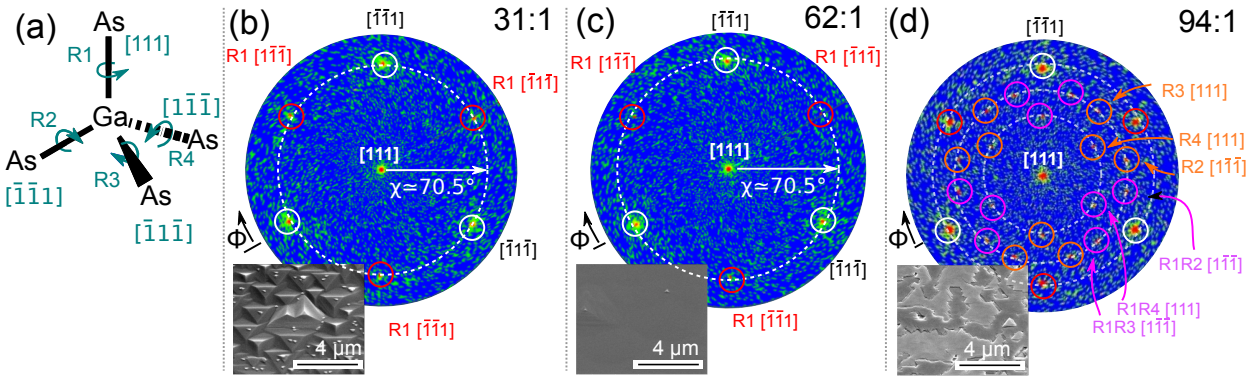

Figure 3: (a) naming scheme of the twinning operators R_i. (b-c) [111] pole figures of samples grown with low (31:1), intermediate (62:1) and high (94:1) As:Ga BEP ratio. Inserts show the corresponding SEM images (reported from Fig. 2). The reflections are indexed using the twin operators R_i and the initial reflection. The circles at constant inclination in (d) are respectively $\chi \simeq 70.5°$, $\chi \simeq 56.3°$ and $\chi \simeq 38.9°$.

450°C) and up to the growth temperature (610°C), we observe a Ge 1×1 pattern, Fig. 1(a), which is characteristic of the Ge surface[11, 10]. The sample is then exposed to As_4 flux at 610°C for a minimum of 5 min, in order to passivate the top Ge surface with As atoms[8, 9, 12]. No modification of the RHEED Ge 1×1 pattern is observed at this step. We then grow a thin GaAs layer (~9 nm, 60 sec growth, 62:1 BEP ratio) which provides a complete coverage of the initial Ge(111) surface. The RHEED pattern remains streaky during the growth of this thin layer, which indicates a planar geometry. The pattern quickly changes from Ge(111) 1×1 to GaAs (111) 2×2 pattern after a few second of GaAs growth. Then, we keep the sample under As_4 flux and we gradually lower the substrate temperature down to 550°C, Fig. 1(b), or increase up to 635°C, Fig. 1(c). We observe that GaAs (111) RHEED pattern remains 2×2 in all the explored temperature range.

We now investigate the effect of As:Ga ratio on the micro-structure GaAs epilayers. We use here ~450 nm thick layers grown at 610°C (~ 50 min growth duration) capped with a thin AlGaAs+GaAs layer (4+4 nm, 610°C), so that the same layer can be analyzed by XRD, TEM and CL. For the low As:Ga BEP ratio (31:1), Fig. 2(a), the GaAs (111) epilayer presents a rough surface with large triangular pyramids, visible by optical microscopy and SEM. Note that a small fraction of the pyramids are rotated by 180° compared to the main population (Fig. 2(a), red circles). These rotated pyramids appear lighter in SEM if the sample is viewed from a specific angle, i.e triangle edge parallel to the scan axis. For intermediate As:Ga BEP ratio (62:1), the epilayer surface is significantly smoother, Fig. 2(b), and surface features are hardly visible. Note that the wide field optical image still shows some large scale roughness including wide dome or pyramidal hillocks. A small region with 180°-rotated pyramids can be found (Fig. 2(b), red circle). For the highest As:Ga BEP ratio (94:1), the epilayer surface is very rough, Fig. 2(c). Instead of the previous features, we now observe a complex pattern of terraces with alternating SEM contrast. Note that this specific SEM contrast is only visible if the sample is viewed from certain angle, similar to the SEM contrast observed on the pyramids in Fig. 2(a).

In Fig. 3, we present the XRD pole figures of the 111 GaAs reflection for the three samples of Fig. 2. Inserts next to each pole figure, Fig. 3(b-d), show the corresponding SEM images (extracted from Fig. 2). The position of each reflection is determined by two angles: ϕ the rotation angle and χ the inclination from the central pole (defined as χ=0). To ease the reflection assignment, we propose in Fig. 3(a) a naming scheme, in which the four possible twins are represented by twinning operators R_i. For cubic GaAs crystals, the twin operators R_i consists in 180° rotations around each bound of the Ga tetrahedron and can be constructed from the corresponding Householder reflection matrices complemented by inversion[13]. The first twin operator is labeled R_1 and corresponds to twin with the [111] as rotation axis. R_1 twinning operates across the (111) growth plane is referred as the *first-order* twinning in the following. The other twinning operators are R_2 for [$\bar{1}\bar{1}$1], R_3 for [$\bar{1}$1$\bar{1}$] and R_4 for [1$\bar{1}\bar{1}$], and referred as *second-order* twinning.

At low and intermediate BEP ratio (62:1), Fig. 3(b-c), we observe the simplest pole figure. We distinguish three types of diffracted beams, the expected central [111] strong reflection, the expected cubic {1$\bar{1}\bar{1}$} strong reflections ($\phi = n \cdot 2\pi/3$, $\chi \simeq 70.5°$ white circles), and a set of three weaker reflections ($\phi = \pi/3 + n \cdot 2\pi/3$,

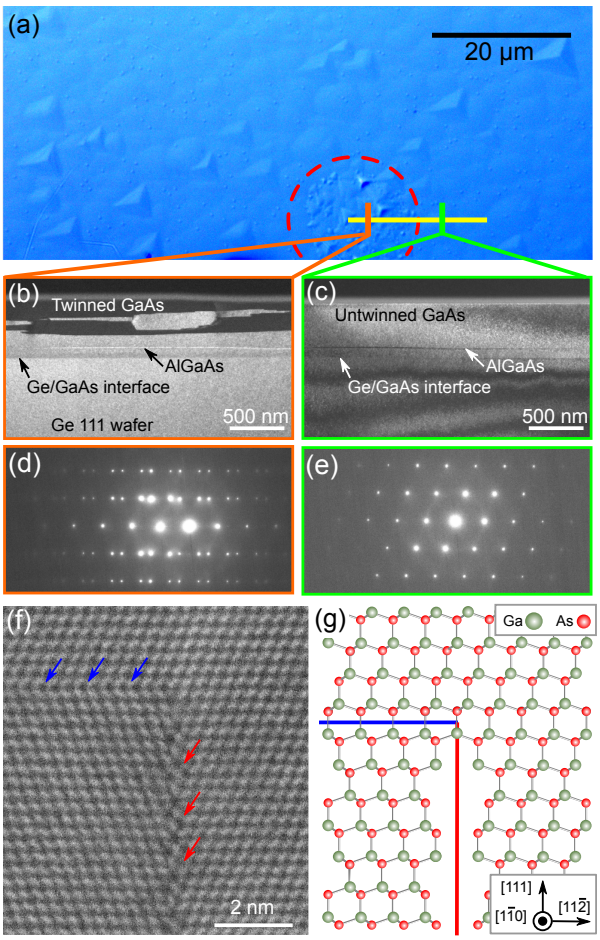

Figure 4: (a) Optical micrograph of the zone selected for cross-section TEM. The yellow line indicates the position of the FIB cut, across a rough patch with 180°-rotated pyramids (red circle). (b) Dark-field TEM from the rough area, orange rectangle in (a), showing twin contrast. (c) Dark-field TEM from the smooth region, green rectangle in (a) observed in the same conditions. (d) TEM diffraction pattern near the [1$\bar{1}$0] zone axis in the twinned area. (e) TEM diffraction pattern in the smooth area. (f) Atomically resolved STEM-HAADF image of a twin boundary. The (111) plane is indicated by blue arrows and the vertical defective boundary by red arrows. (g) Corresponding atomic structure for two twinned GaAs cubic crystals.

$\chi \simeq 70.5°$, red circles) which corresponds to the $\{1\overline{1}\overline{1}\}$ reflection family after the application of the R_1 operator. The later transforms the 3-fold symmetry of the standard GaAs 111 pole figure into a pattern with 6-fold symmetry. At the lowest BEP ratio (31:1), Fig. 3(b), R_1 twinning is slightly more pronounced that at intermediate BEP ratio (62:1).

At the highest BEP ratio (94:1), Fig. 3(d), the pole figure is very dense. In addition to all the reflections previously identified in Fig. 3(b, red and white circles), we observe two additional sets of reflections. The first set is marked by orange circles and consists in reflections obtained after *second-order* twinning ($R_{j,\ j\neq 1}$) on all the possible {111} directions. The second set (purple circles) is obtained after the application of the R_1 operator on the previous set, so that the pole figure recovers a 6-fold symmetry. A few additional weak reflection are visible and ascribed to other multiple-order twinning combinations ($R_j \cdot R_i$).0

We now analyze by TEM a sample grown using the intermediate (64:1) BEP ratio, which yields the smoothest surface, Fig. 2(b), and the simplest XRD pole figure, Fig. 3(c). The sample consists in a GaAs buffer layer (~90 nm), a thin AlGaAs layer (~9 nm) and thick GaAs layer (~450 nm). The AlGaAs marker layer permits to assess the smoothness of the layer and gives a reference position in the TEM cross-section images. As the epilayer is mostly defect free, see Fig. 2(b), we use focused ion beam (FIB) to select a zone of interest at the interface between the 'smooth' surface and a 'rougher' patch with 180°-rotated pyramids, Fig. 4(a).

The TEM dark field contrast in Fig. 4(b)(c) is obtained by selecting a diffraction spot specific to one of the two twin orientations. In these imaging conditions, the Ge substrate and the main section of the GaAs epilayer appear in bright color, while the GaAs twinned crystal is dark. In the cross section from the rougher patch, Fig. 4(b), we observe large twin domains with a complex internal structure. In the smooth region, Fig. 4(c), we observe a single continuous crystal all across the layers with no visible defect. The TEM diffraction patterns near the [1$\bar{1}$0] zone axis, Fig. 4(d-e), confirm respectively the presence and absence of twinned domains.

Figure 4(f) shows the atomic arrangement around a twin boundary using scanning-TEM (STEM) high angle annular dark field (HAADF) imaging. The corresponding atomic configuration is sketched Fig. 4(g) for two GaAs crystals related the twin operator R_1. The (111) growth plane, which is the plane of rotation in R_1, is marked by blue arrows and line in Fig. 4(f-g). The complete twin boundary consists in the (111) plane and a defective vertical plane, possibly (11$\bar{2}$), indicated by red arrows and line in Fig. 4(f-g).

In Fig. 5, we use SEM-ESBD to investigate the crystal orientation of top GaAs surface at small and large scales. The Fig. 5(a) shows the SEM and corresponding EBSD map of a small rough patch with 180°-rotated pyramids from the sample previously characterized by TEM (Fig. 4). We confirm by EBSD the twinning of the crystal (orange vs. purple color). As both materials are [111] oriented, we use here a color scale related to the Euler angles with respect to the EBSD detector

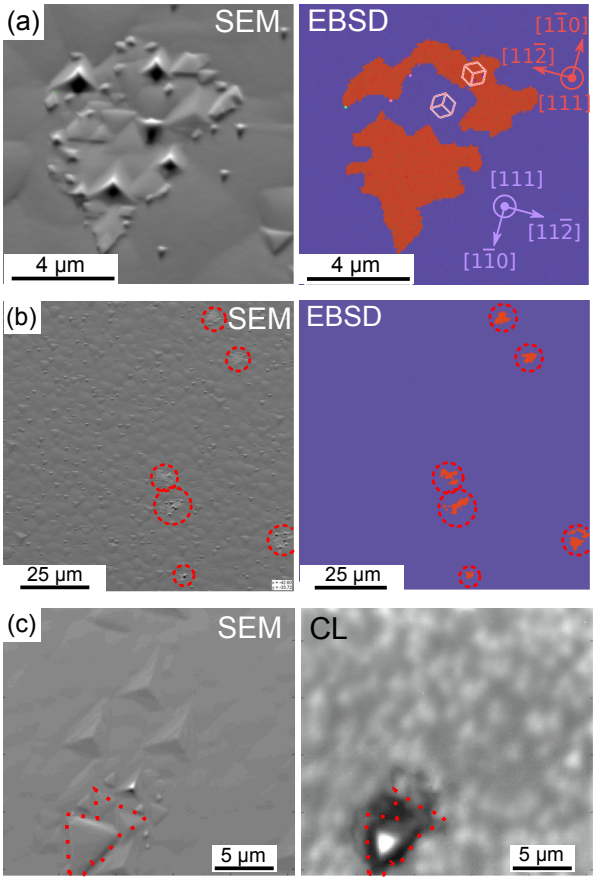

Figure 5: (a) SEM-EBSD characterization of a small rough area showing the emergence of two small twinned domains (orange) in the main layer (purple). The orientation of the crystal is indicated by a color relative to its Euler angles with the EBSD detector. The projected cubic unit cell is shown as a pink polygon. Crystal orientations are labeled with matching colors. (b) Large scale SEM-ESBD characterization. Rough and twin area are indicated by red circles. The EBSD color scale is the same as in (a). (c) Room temperature SEM-CL (6 kV) of a small twinned area. The CL color scale is proportional to the integrated GaAs peak intensity. The dotted red line indicates the estimated position of the defective twin boundary.

to differentiate their respective orientations. The twinning relation (R_1 operator) is visible from 180°-rotation of the crystal axis, indicated by the respective position of the pink polygons (projected unit cell) and by the axis labels. We note that the boundary of the twinned domains (seen by EBSD) nearly coincides with that of the rougher patch (seen by SEM). At the large scale, Fig. 5(b), we observe that the sample is mostly twin-free and that the positions of all small twinned domains (orange color in EBSD) match exactly that of the rough patches visible by SEM (red circles).

Using SEM-CL, Fig. 5(c), we evaluate the impact of twinned domains on the optical properties of the GaAs epilayer. We focus on a small twinned domain, which emerges at the surface with 180° rotated pyramids (SEM image). The corresponding CL map obtained from the integration of the GaAs emission peak at room temperature (~300K) shows some small features in the smooth area and a large drop of signal near the expected position of the twin boundary (red dotted line, estimated from the pyramid orientation in the SEM image).

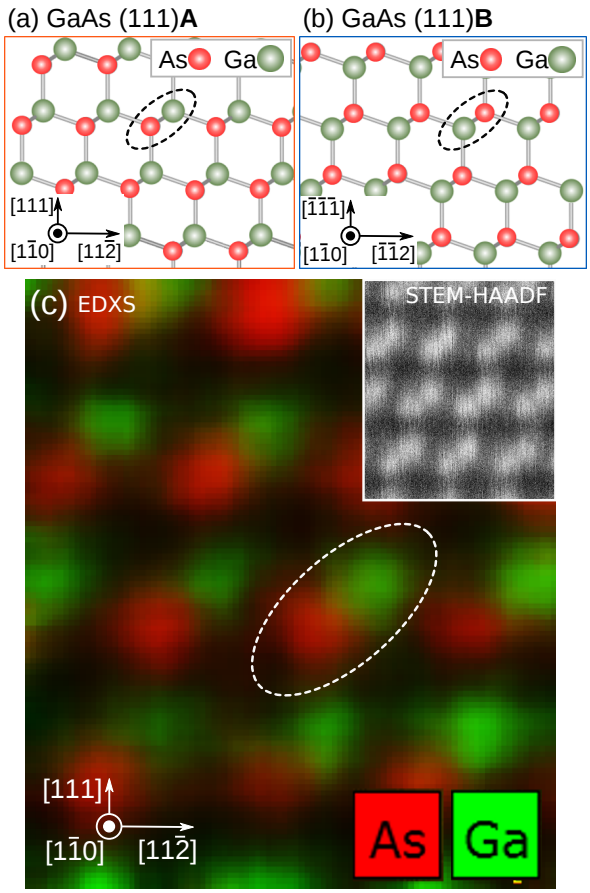

Figure 6: Schematic of (a) GaAs(111)A, and (b) GaAs(111)B atomic structure. (c) Atomically resolved STEM-EDX of the GaAs layer grown at intermediate As:Ga ratio (62:1), viewed along the [1$\bar{1}$0] zone axis. Insert shows the corresponding STEM-HAADF image.

In Fig. 6, we investigate the polarity of the GaAs smooth epilayer grown at intermediate BEP ratio (62:1), previously analyzed in Fig. 3 & 4. Fig. 6 (a) and (b) show the crystal structure of GaAs(111)B and GaAs(111)A respectively. For GaAs(111)B, Fig. 6(a), the As atom terminates the As-Ga dumbbell (dotted circle) while it is opposite for GaAs(111)A, Fig. 6(b). The direct comparison with the atomically resolved STEM-EDX map, Fig. 6(c), demonstrates that the GaAs epi-

layer has the (111)A orientation. Note that twin defects, see Fig. 4, do not change the layer polarity.

3. Discussion

3.1. Antiphase and twin boundaries

Whereas the GaAs/Ge(111) growth is immune from antiphase inclusions[10], it is very prone to twinning. As seen by TEM (Fig. 4) and EBSD (Fig. 5), twinned domains are three-dimensionnal inclusions with two types of boundaries. The first one is the (111) twin plane itself (Fig. 4(e), blue line) and is simply a (111) stacking fault. The second type of boundary is contained in the $(11\bar{2})$ plane (Fig. 4(e), red line). The actual atomic structure of this interface is not detailed here but it cannot consist only in standard III-V bounds for symmetry reason. The CL results, Fig. 5(c), show clearly that this vertical interface present large densities of non-radiative recombination centers active at room temperature. On the opposite, the stacking fault defect in the (111) plane is reported to create a type II band alignment with various radiative components[14, 15].

Despite the different defects and crystal orientations, the defective non-radiative twin-boundaries observed in GaAs(111) heteroepitaxy behave very similarly to the vertical antiphase boundaries found in GaAs(100) layers[16, 17]. Both defects run though the epilayer thickness and hold large densities of non-radiative recombination centers. The reduction of twin defect density in (111) epilayers is thus as critical as the removal of antiphase domains in III-V (100) heteroepitaxy.

The main difference between the formation of antiphase and twinned domains is that twining only relates to the possibility of creating stacking fault-like defects. Therefore, twinned domains can form in any (111) oriented III-V epilayers, independently of the polar (III-V/III-V) or non-polar (III-V/IV-IV) nature of the substrate, and even if the epilayer and its substrate are very close chemically[18] or identical[19].

3.2. Reduction in twin densities

With such a detrimental effect of the twin boundaries on the layer optical quality, it is very important to limit the density of twinned domain in GaAs(111) epilayers. Twinning is a common problem in the heteroepitaxy of (111) oriented III-V compounds. Recent work by Koppka *et al.* reports twin defects at the GaP/Si (111) interface, which can be limited using an As-treatment of the Si (111) surface and a low temperature nucleation layer prior to the GaP growth[20]. Closer to our work is that of Kajikawa *et al.* [12] on the MBE growth GaAs/Ge(111) using a GaSb buffer to minimize the twin density, in line with other attempts using Sb on GaAs/Si(111)[21] and Sb pretreatment in GaSb/Si(111)[22].

The assessment of the epilayer 'quality' with respect to twin defects is not an easy task. XRD results, Fig. 3, only indicate the volume fraction of the twinned phase. Yet, the critical parameter is the density of (non-radiative) twin boundaries which emerge at the surface. Here, we first use TEM to associate specific surface defect with twinned domains, Fig. 4. Then we use SEM-EBSD to validate this approach at small and large scale, Fig. 5, so that simple optical images can be used to evaluate the layer quality at the wafer scale, Fig. 2. This methodology gives us confidence that the layers grown at intermediate (62:1) As:Ga BEP ratio are mostly twin-free.

In contrast to Kajikawa *et al.* [12], we show that the twin density of GaAs/Ge(111) can be reduced by tuning the As:Ga ratio, see Fig. 3, without the addition of any other extra chemical element. The main difference with ref.[12] is the use of higher As_4:Ga BEP ratio (60 instead of 15) and higher substrate temperature (610°C instead of 550°C).

From figures 2 and 3, we infer that there is an optimum value of the As:Ga ratio, which is rather unexpected. At low As:Ga ratio (31:1) the surface is rough with some trace of first order twinning (R_1), while it is much smoother and slightly less twinned at intermediate As:Ga ratio (62:1). The later is coherent with existing studies on the homoepitaxy of GaAs(111)A by MBE[23, 24, 25]. Careful observation of the Figure 1 in ref.[25] shows that small twinned domains form at 600° and low As:Ga ratio, while no twins are observed for higher As:Ga ratios, which is similar to our results.

After the initial improvement with increasing V:III ratio (31:1↦62:1), we observe a stark degradation of the surface morphology, Fig. 2, and layer microstructure, Fig. 3, at higher As:Ga BEP ratio (94:1). Such optimal As:Ga ratio is not found in homoepitaxial studies[23, 24, 25], which only report a monotonic improvement. A likely culprit is the degradation of the GaAs/Ge(111) interface at the initial stages of the growth, which leads to the growth of large twinned domains.

3.3. Polarity

For device application, the choice of polarity from GaAs(111)B to (111)A has strong implications as the standard n-type doping using Si impurities usually leads to a severe compensation effect in GaAs (111)A layers[26, 27].

As seen above, our GaAs epilayers have very similar morphologies to those fabricated by homoepitaxial growth on GaAs(111)A substrates[25]. The surface reconstructions observed by RHEED, Fig. 1, also hint at a GaAs(111)A polarity. We only observe the 2×2 pattern, independently of the substrate temperature between 550°C and 635°C, which is the expected behavior of GaAs(111)A surfaces, whereas GaAs(111)B should exhibit $\sqrt{19} \times \sqrt{19}$ or 1×1 static reconstructions in this temperature range[28]. The detailed TEM analysis using EDX, Fig. 6, confirms that the epilayer grown at intermediate As:Ga ratio (62:1) indeed have the GaAs(111)A orientation. Further analysis by EBSD, Fig. 5, shown that the epilayer is homogeneous on a large scale (> 100 μm) and only present twin defects, which do not alter the layer polarity.

The homogeneous nucleation of GaAs with the (111)A polarity is rather surprising as it conflicts with the accepted growth model. In the As-reconstructed surface of Ge(111) proposed by Bringans *et al.* , As atoms get inserted inside the Ge(111) monolayer so that the final surface does not present any dangling bounds[8, 9]. The geometry of these As atoms directly imposes a GaAs(111)B polarity for subsequent GaAs layer, see Fig. 7(a). This supposedly unambiguous determination of GaAs polarity on Ge(111) was used in lattice-reversal experiment in which GaAs(111)B epilayers are grown on GaAs(111)A wafers after the insertion of a Ge buffer[11]. Considering the reported strong interaction of Ge(111) with As-atom, a possible solution to obtain the (111)A polarity is an alternative As-surface termination, Fig. 7(b), in which the As atoms simply bounds to the Ge(111) monolayer, similar to the hydrogen passivation of Ge(111) using HF or H_2[29, 30].

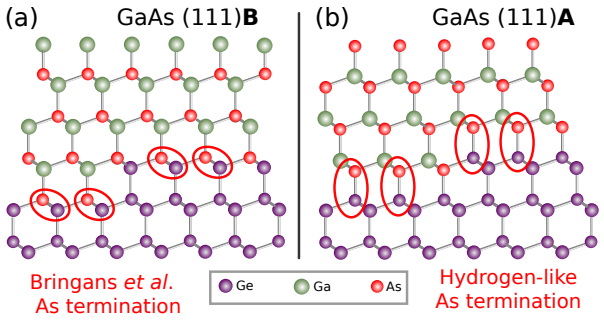

Figure 7: (a) Schematic of the As-surface termination of Ge(111) reported by Bringans *et al.* [9], leading the growth of GaAs(111)B epilayers. (b) Proposed 'hydrogen-like' As termination leading the growth of GaAs(111)A epilayers.

Excepting ancient work reporting pure GaAs (111)B or GaAs(111)A polarity on Ge(111) by chemical vapor deposition depending on the presence of oxygen contamination[31], the present study is the only recent report of pure phase GaAs(111)A / Ge(111). While we cannot exclude a potential contamination of the Ge(111) surface, we note that this contamination must be homogeneous over the whole sample (i.e no mixture of GaAs(111)B and (111)A is observed), it is also not visible by RHEED (see Fig. 1) and it occurs despite the low base pressure in the MBE growth chamber (< 10^{-10} Torr). Similarly, the chemical analysis of the epilayer using TEM-EDX, see Supplementary Information S1, does not reveals any increased oxygen content at the GaAs/Ge(111) interface. The robust formation of pure phase GaAs(111)A or GaAs(111)B is nonetheless very interesting as potential surface treatments of the initial Ge(111) surface could determine uniquely the epilayer polarity.

4. Conclusion

We demonstrate the first twin-free and defect-free growth of GaAs(111)A epilayers on nominal Ge(111) wafers by MBE. While the observed GaAs(111)A polarity is unexpected, it is nonetheless homogeneous and robust. Compared to the complex growth procedures used in the case of GaAs/Ge(100), the growth of defect-free GaAs on Ge(111) can be carried in a single step at 610°C. No antiphase domains form on the Ge(111) surface but twinned domains appear if the As:Ga ratio is not adapted. Some twin boundaries hold large number of non-radiative recombination centers and it is critical to limit their density. The later can be minimized by the careful tuning of the As:Ga flux ratio during growth, without the use of any additional chemical element or buffer layer.

Acknowledgement

The authors thank the Institut Photovoltaique d'Ile de France (IPVF) for financial support under framework project E.3. The authors also acknowledge ANR Investissement d'Avenir program (TEMPOS Project ANR-10-EQPX-50) for having funded the acquisition of the NANOTEM platform and the TEM-STEM (FEI Titan Themis) used in this work.

References

[1] D. Gerthsen, D. Biegelsen, F. Ponce, J. Tramontana, Misfit dislocations in gaas heteroepitaxy on (001) Si, Journal of Crystal Growth 106 (2-3) (1990) 157–165 (Nov. 1990). doi:10.1016/0022-0248(90)90059-t.

[2] V. K. Yang, M. Groenert, C. W. Leitz, A. J. Pitera, M. T. Currie, E. A. Fitzgerald, Crack formation in GaAs heteroepitaxial films on Si and SiGe virtual substrates, Journal of Applied Physics 93 (7) (2003) 3859–3865 (Apr. 2003). doi:10.1063/1.1558963.

[3] C. Merckling, N. Waldron, S. Jiang, W. Guo, O. Richard, B. Douhard, A. Moussa, D. Vanhaeren, H. Bender, N. Collaert, M. Heyns, A. Thean, M. Caymax, W. Vandervorst, Selective area growth of InP in shallow trench isolation on large scale Si(001) wafer using defect confinement technique, Journal of Applied Physics 114 (3) (2013) 033708 (Jul. 2013). doi:10.1063/1.4815959.

[4] M. Holland, M. van Dal, B. Duriez, R. Oxland, G. Vellianitis, G. Doornbos, A. Afzalian, T.-K. Chen, C.-H. Hsieh, P. Ramvall, T. Vasen, Y.-C. Yeo, M. Passlack, Atomically flat and uniform relaxed III-V epitaxial films on silicon substrate for heterogeneous and hybrid integration, Scientific Reports 7 (1) (Nov. 2017). doi:10.1038/s41598-017-15025-0.

[5] I. Lucci, S. Charbonnier, L. Pedesseau, M. Vallet, L. Cerutti, J.-B. Rodriguez, E. Tourni, R. Bernard, A. Ltoublon, N. Bertru, A. L. Corre, S. Rennesson, F. Semond, G. Patriarche, L. Largeau, P. Turban, A. Ponchet, C. Cornet, Universal description of III-V/Si epitaxial growth processes, Physical Review Materials 2 (6) (Jun. 2018). doi:10.1103/physrevmaterials.2.060401.

[6] P. Pukite, P. Cohen, Suppression of antiphase domains in the growth of GaAs on Ge(100) by molecular beam epitaxy, Journal of Crystal Growth 81 (1-4) (1987) 214–220 (Feb. 1987). doi:10.1016/0022-0248(87)90393-9.

[7] R. M. Sieg, S. A. Ringel, S. M. Ting, E. A. Fitzgerald, R. N. Sacks, Anti-phase domain-free growth of GaAs on offcut (001) Ge wafers by molecular beam epitaxy with suppressed Ge outdiffusion, Journal of Electronic Materials 27 (7) (1998) 900–907 (Jul. 1998). doi:10.1007/s11664-998-0116-1.

[8] R. D. Bringans, Arsenic passivation of Si and Ge surfaces, Critical Reviews in Solid State and Materials Sciences 17 (4) (1992) 353–395 (Jan. 1992). doi:10.1080/10408439208242194.

[9] R. D. Bringans, R. I. G. Uhrberg, R. Z. Bachrach, J. E. Northrup, Arsenic-terminated Ge(111): An ideal 111 surface, Physical Review Letters 55 (5) (1985) 533–536 (Jul. 1985). doi:10.1103/physrevlett.55.533.

[10] T. Kawai, H. Yonezu, Y. Yamauchi, M. Lopez, K. Pak, W. Krner, Initial growth process of GaAs on Ge substrate and pseudomorphic Si interlayer, Journal of Crystal Growth 127 (1-4) (1993) 107–111 (Feb. 1993). doi:10.1016/0022-0248(93)90587-m.

[11] S. Koh, T. Kondo, Y. Shiraki, R. Ito, GaAs/Ge/GaAs sublattice reversal epitaxy and its application to nonlinear optical devices, Journal of Crystal Growth 227-228 (2001) 183–192 (Jul. 2001). doi:10.1016/s0022-0248(01)00660-1.

[12] Y. Kajikawa, Y. Son, H. Hayase, H. Ichiba, R. Mori, K. Ushirogouchi, M. Irie, Suppression of twin generation in the growth of GaAs on Ge(111) substrates, Journal of Crystal Growth 477 (2017) 40–44 (Nov. 2017). doi:10.1016/j.jcrysgro.2016.12.062.

[13] E. Uccelli, J. Arbiol, C. Magen, P. Krogstrup, E. Russo-Averchi, M. Heiss, G. Mugny, F. Morier-Genoud, J. Nygård, J. R. Morante, A. F. i Morral, Three-dimensional multiple-order twinning of self-catalyzed GaAs nanowires on Si substrates, Nano Letters 11 (9) (2011) 3827–3832 (Sep. 2011). doi:10.1021/nl201902w.

[14] B. Loitsch, J. Winnerl, G. Grimaldi, J. Wierzbowski, D. Rudolph, S. Morktter, M. Dblinger, G. Abstreiter, G. Koblmller, J. J. Finley, Crystal phase quantum dots in the ultrathin core of GaAsAlGaAs coreshell nanowires, Nano Letters 15 (11) (2015) 7544–7551 (Oct. 2015). doi:10.1021/acs.nanolett.5b03273.

[15] N. Vainorius, D. Jacobsson, S. Lehmann, A. Gustafsson, K. A. Dick, L. Samuelson, M.-E. Pistol, Observation of type-ii recombination in single wurtzite/zinc-blende GaAs heterojunction nanowires, Physical Review B 89 (16) (Apr. 2014). doi:10.1103/physrevb.89.165423.

[16] S. N. G. Chu, S. Nakahara, S. J. Pearton, T. Boone, S. M. Vernon, Antiphase domains in GaAs grown by metalorganic chemical vapor deposition on silicon-on-insulator, Journal of Applied Physics 64 (6) (1988) 2981–2989 (Sep. 1988). doi:10.1063/1.341561.

[17] K. Nauka, G. A. Reid, Z. Liliental-Weber, Electron beam induced current and cathodoluminescence imaging of the antiphase domain boundaries in GaAs grown on Si, Applied Physics Letters 56 (4) (1990) 376–378 (Jan. 1990). doi:10.1063/1.102790.

[18] Y. R. Chen, L. C. Chou, Y. J. Yang, H. H. Lin, Twinning in GaAsSb grown on (111)B GaAs by molecular beam epitaxy, Journal of Physics D: Applied Physics 46 (3) (2012) 035306 (Dec. 2012). doi:10.1088/0022-3727/46/3/035306.

[19] Y. Park, M. J. Cich, R. Zhao, P. Specht, E. R. Weber, E. Stach, S. Nozaki, Analysis of twin defects in GaAs(111)B molecular beam epitaxy growth, Journal of Vacuum Science & Technology B: Microelectronics and Nanometer Structures 18 (3) (2000) 1566 (2000). doi:10.1116/1.591427.

[20] C. Koppka, A. Paszuk, M. Steidl, O. Supplie, P. Kleinschmidt, T. Hannappel, Suppression of rotational twin formation in virtual GaP/Si(111) substrates for III-V nanowire growth, Crystal Growth & Design 16 (11) (2016) 6208–6213 (Oct. 2016). doi:10.1021/acs.cgd.6b00541.

[21] O. Morohara, H. Geka, Y. Moriyasu, N. Kuze, Sb irradiation effect on growth of GaAs thin film on Si (111) substrate, Journal of Crystal Growth 378 (2013) 113–116 (Sep. 2013). doi:10.1016/j.jcrysgro.2013.02.002.

[22] H. Toyota, A. Okabe, T. Endoh, Y. Jinbo, N. Uchitomi, Study of Sb template for heteroepitaxial growth of GaSb thin film on Si(111) substrate, Journal of Crystal Growth 378 (2013) 129–133 (Sep. 2013). doi:10.1016/j.jcrysgro.2012.12.072.

[23] L. Esposito, S. Bietti, A. Fedorov, R. Ntzel, S. Sanguinetti, Ehrlich-schwbel effect on the growth dynamics of GaAs(111)A surfaces, Physical Review Materials 1 (2) (Jul. 2017). doi:10.1103/physrevmaterials.1.024602.

[24] K. Sato, M. R. Fahy, B. A. Joyce, The growth of high quality GaAs on GaAs (111)A, Japanese Journal of Applied Physics 33 (Part 2, No. 7A) (1994) L905–L907 (Jul. 1994). doi:10.1143/jjap.33.l905.

[25] J. Ritzmann, R. Schott, K. Gross, D. Reuter, A. Ludwig, A. D. Wieck, Overcoming ehrlich-schwbel barrier in (111)A GaAs molecular beam epitaxy, Journal of Crystal Growth 481 (2018) 7–10 (Jan. 2018). doi:10.1016/j.jcrysgro.2017.10.029.

[26] K. Sato, M. Fahy, M. Ashwin, B. Joyce, Silicon incorporation behaviour in GaAs grown on GaAs (111)A by molecular beam epitaxy, Journal of Crystal Growth 165 (4) (1996) 345–350 (Aug. 1996). doi:10.1016/0022-0248(96)00219-9.

[27] N. G. Yaremenko, M. V. Karachevtseva, V. A. Strakhov, G. B. Galiev, V. G. Mokerov, Photoluminescence of Si-doped GaAs epitaxial layers, Semiconductors 42 (13) (2008) 1480–1486 (Dec. 2008). doi:10.1134/s1063782608130058.

[28] D. A. Woolf, D. I. Westwood, R. H. Williams, The homoepitaxial growth of GaAs(111)A and (111)B by molecular beam epitaxy: an investigation of the temperature-dependent surface reconstructions and bulk electrical conductivity transitions, Semiconductor Science and Technology 8 (6) (1993) 1075–1081 (Jun. 1993). doi:10.1088/0268-1242/8/6/014.

[29] T. Deegan, G. Hughes, An X-ray photoelectron spectroscopy study of the HF etching of native oxides on Ge(111) and Ge(100) surfaces, Applied Surface Science 123-124 (1998) 66–

70 (Jan. 1998). doi:10.1016/s0169-4332(97)00511-4.

[30] K. T. Wong, Y.-G. Kim, M. P. Soriaga, B. S. Brunschwig, N. S. Lewis, Synthesis and characterization of atomically flat methyl-terminated Ge(111) surfaces, Journal of the American Chemical Society 137 (28) (2015) 9006–9014 (Jul. 2015). doi:10.1021/jacs.5b03339.

[31] L. C. Bobb, H. Holloway, K. H. Maxwell, E. Zimmerman, Oriented growth of semiconductors. iii. growth of gallium arsenide on germanium, Journal of Applied Physics 37 (13) (1966) 4687–4693 (Dec. 1966). doi:10.1063/1.1708118.

Supplementary Information

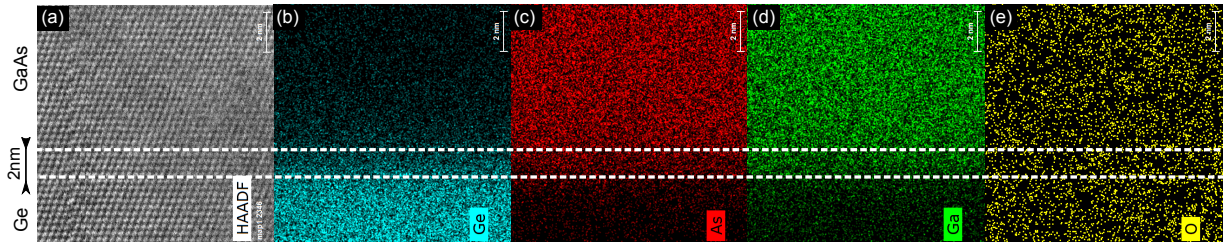

Figure S1 : Chemical analysis of the GaAs(111)A/Ge(111) interface using STEM-HAADF (a) and STEM-EDX (b-e) for the Ga, As, Ge and O elements. The white dashed lines delimits the probable location of the initial GaAs/Gee growth interface.

The Figure S1 shows the chemical analysis of the GaAs/Ge interface using STEM-HAADF and EDX. The exact position of the initial GaAs/Ge(111) growth interface is lost due to the strong inter-diffusion of Ge, Ga and As, which extends over ~2 nm (5-6 ML) in our growth conditions. Yet, the approximative location of the initial GaAs/Ge interface is contained between the two white dashed lines. From Fig. S1(e), we see that the oxygen content is homogeneous over the whole cross section, without any visible variation around the estimated position of the initial interface. Similarly, the HAADF image show no variation of contrast near or across the approximative position of Ge/GaAs interface.